Inorganic Chemistry

Article

pubs.acs.org/IC

Syntheses, Crystal Structures, Optical and Theoretical Studies of the Actinide Thiophosphates $SrU(PS_4)_2$, $BaU(PS_4)_2$, and $SrTh(PS_4)_2$

Adel Mesbah,[†,‡] Jai Prakash,[†] Jessica C. Beard,[†] Sébastien Lebègue,[§] Christos D. Malliakas,[†] and James A. Ibers*,[†]

[†]Department of Chemistry, Northwestern University, 2145 Sheridan Road, Evanston, Illinois 60208-3113, United States

[‡]ICSM, UMR 5257 CEA/CNRS/UM2/ENSCM, Site de Marcoule—Bât. 426, BP 17171, 30207 Bagnols-sur-Cèze cedex, France

[§]Laboratoire de Cristallographie, Résonance Magnétique et Modélisations (CRM2, UMR CNRS 7036), Institut Jean Barriol, Université de Lorraine, BP 239, Boulevard des Aiguillettes, 54506 Vandoeuvre-lès-Nancy, France

Supporting Information

ABSTRACT: Three new actinide thiophosphates, $SrU(PS_4)_2$, $BaU(PS_4)_2$, and $SrTh(PS_4)_2$, have been synthesized by high-temperature solid-state methods, and their crystal structures were determined from single-crystal X-ray diffraction studies. These three isostructural compounds crystallize in a new structure type in space group D_{4h}^{13}-$P4_2/mbc$ of the tetragonal system. Their structure features infinite one-dimensional chains of $^1_\infty[An(PS_4)_2{}^{2-}]$ anions (An = U or Th). Each An atom is coordinated by eight S atoms in a bicapped trigonal prism, and each P atom is tetrahedrally bonded to four S atoms. The compounds are readily charge balanced as $Ak^{2+}An^{4+}(P^{5+}(S^{2-})_4)_2$. Optical studies on single crystals of $SrU(PS_4)_2$ and $BaU(PS_4)_2$ as well as ground single crystals of $SrTh(PS_4)_2$ revealed a direct band gap of 2.13(2) eV and an indirect band gap value of 1.99(2) eV for $SrU(PS_4)_2$ and a direct and indirect gap of about 2.28(2) eV for $BaU(PS_4)_2$. $SrTh(PS_4)_2$ has a relatively large band gap of 3.02(2) eV. DFT calculations for $SrU(PS_4)_2$ and $BaU(PS_4)_2$ using the HSE functional predict both compounds to be antiferromagnetic and have very similar electronic structures with band gaps of 2.7 eV. The band gap calculated for $SrTh(PS_4)_2$ is 3.2 eV.

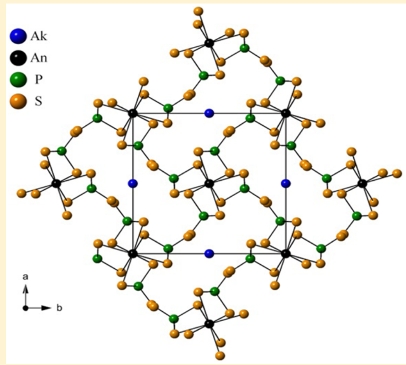

■ INTRODUCTION

The chemistry of the actinide phosphates is of great interest owing to its involvement in the nuclear fuel cycle, particularly in the management of nuclear wastes. A variety of phosphate-based compounds have been identified as potential matrices for nuclear wastes because these compounds present remarkable chemical flexibility that enables the incorporation of high amounts of U and Th and minor amounts of the heavier actinides, especially Am and Cm. Their high durability and stability under extreme conditions of radiation, pressure, and temperature are desirable properties for such applications. Among these phosphates, the monazites $LnPO_4$ (Ln = lanthanide)[1−3] and thorium phosphate-diphosphate (PDT) have proved to be very important.[4,5]

Interest in potential matrices may have been an impetus for exploratory syntheses to find new actinide phosphates. In any event in recent years a number of new compounds have been found. To take the uranium(IV) phosphates as an example, now known are $U(UO_2)_2(PO_4)_2$,[6] $U_2(PO_4)(P_3O_{10})$,[7] $U_2O(PO_4)_2$,[8] and α-$U(P_2O_7)$.[9] Similar activity in actinide phosphosulfide compounds has led to a variety of new compounds. Examples include the ternaries $UP_{1-x}S_x$,[10] UPS,[11] ThP_2S_6,[12] UP_2S_6,[13] $U(P_2S_6)_2$,[13] UP_2S_7,[13,14] UP_2S_9,[14] $U_3(PS_4)_4$,[13] $Np(PS_4)$[15] and $Np(P_2S_6)_2$;[15] the quaternaries $A_{11}U_7(PS_4)_{13}$ (A = K, Rb),[16] $A_{11}Np_7(PS_4)_{13}$ (A = K, Rb),[15] $CsLiU(PS_4)_2$,[17] $Cs_8U_5(P_3S_{10})_2(PS_4)_6$,[18] $A_5An(PS_4)_3$ (A = K, Rb, Cs and An = U, Th),[18] $K_3Pu(PS_4)_2$,[19] $APuP_2S_7$ (A = K, Rb, Cs),[19] and $Cs_4Th_2P_6S_{18}$;[20] and even the quintary $A_6U_3Sb_2P_8S_{32}$.[21] The greater diversity of stoichiometries among the phosphosulfides arises from the ability of the chalcogens (Q = S, Se, Te) to form Q−Q bonds and also to condense to polymeric substructures, for example, PQ_3, P_2Q_6, P_2Q_{10}, P_4Q_{13}, P_6Q_{12}, and PQ_6.[18,22−25]

Here we report the syntheses, crystal structures, as well as optical and theoretical results for three new isostructural compounds $SrU(PS_4)_2$, $BaU(PS_4)_2$, and $SrTh(PS_4)_2$. To our knowledge, these are the first actinide phosphosulfides involving alkaline-earth metals.

■ EXPERIMENTAL METHODS

Syntheses and Analyses. ***Caution!*** *^{232}Th and depleted U are α-emitting radioisotopes and as such are considered a health risk. Their use requires appropriate infrastructure and personnel trained in the handling of radioactive materials.*

The following reactants were used as supplied: Ba (Johnson Matthey, 99.5%), Sr (Aldrich, 99.0%), Th (MP Biomedicals, 99.1%), P_2S_5 (Aldrich, 99%), S (Mallinckrodt, 99.6%), and CsCl (Aldrich, 99.9%). Depleted U powder was obtained by hydridization of U metal

Received: January 9, 2015
Published: February 25, 2015

DOI: 10.1021/acs.inorgchem.5b00071
Inorg. Chem. 2015, 54, 2970−2975

(IBI Laboratories) in a modification[26] of a previous procedure.[27] The reactants were weighed and transferred into 6 mm carbon-coated silica-tubes inside an Ar-filled drybox. These silica tubes containing reaction mixtures were then evacuated to 10^{-4} Torr, flame-sealed, and heated in a computer controlled furnace. Semiquantitative analyses of the resultant products were obtained by means of electron dispersive X-ray (EDX) studies using an Hitachi S-3400 SEM.

Synthesis of $SrU(PS_4)_2$. $SrU(PS_4)_2$ was obtained by direct combination of Sr (7.36 mg, 0.085 mmol), U (20 mg, 0.085 mmol), P_2S_5 (19.15 mg, 0.085 mmol), and S (16.17 mg, 0.504 mmol). The reaction mixture was heated to 1123 K in 48 h, held there for 96 h, and then cooled at 2.5 K/h to 673 K, and finally to 298 K in 12 h. The reaction produced orange needles of $SrU(PS_4)_2$ (Sr:U:P:S ≈ 1:1:2:8) in about 70 wt % yield as well as black block-shaped crystals of UP_2S_7[13,14] (U:P:S ≈ 1:2:7).

Synthesis of $BaU(PS_4)_2$. $BaU(PS_4)_2$ was obtained in a reaction of Ba (35 mg, 0.255 mmol), U (20.23 mg, 0.085 mmol), P_2S_5 (56.61 mg, 0.255 mmol), S (16.35 mg, 0.51 mmol), and excess CsCl flux (100 mg). The reaction mixture was heated to 1053 K in 24 h, held there for 12 h, then cooled to 773 K in 90 h and held there for 96 h. The reaction mixture was then cooled to 473 K in 90 h, and finally the furnace was turned off. Orange needles of $BaU(PS_4)_2$ (Ba:U:P:S ≈ 1:1:2:8) were obtained in about 10 wt % yield. The major product comprised black block-shaped crystals of UP_2S_7[13,14] (U:P:S ≈ 1:2:7).

Synthesis of $SrTh(PS_4)_2$. $SrTh(PS_4)_2$ was synthesized by the reaction of Sr (7.36 mg, 0.085 mmol), Th (20 mg, 0.085 mmol), P_2S_5 (19.15 mg, 0.085 mmol), S (11.05 mg, 0.345 mmol), and excess CsCl flux (100 mg). The reaction mixture was heated to 1123 K in 48 h, annealed at that temperature for 96 h, and then the furnace was turned off. Yellow needles of $SrTh(PS_4)_2$ (Sr:Th:P:S ≈ 1:1:2:8) were obtained in approximately 70 wt % yield accompanied by a small amount of block-shaped crystals of SrS (Sr:S ≈ 1:1).[28]

Crystal Structure Determinations. Single-crystal X-ray data for $BaU(PS_4)_2$, $SrU(PS_4)_2$, and $SrTh(PS_4)_2$ were collected at 100(2) K using a Bruker APEX2 Kappa diffractometer. Cu Kα (λ = 1.54178 Å) radiation was used for $BaU(PS_4)_2$ (crystal-to-detector distance = 40 mm), and Mo Kα (λ = 0.710 73 Å) radiation was used for $SrU(PS_4)_2$ and $SrTh(PS_4)_2$ (crystal-to-detector distance = 60 mm). For all compounds the data collection strategy consisted of a combination of ω and φ scans as obtained by the use of the algorithm COSMO in APEX2[29] with steps of 0.3° and counting time of 10 s/frame. Recorded data were indexed, refined, and integrated by SAINT in the APEX2 package.[29] Face-indexed absorption, incident beam, and decay corrections were performed with the use of the program SADABS.[30] The precession images of these data showed no indication of super cells or modulation. The crystal structures were solved and refined with the use of programs in the SHELXTL 2014 package.[30,31] The atomic positions were standardized by the program STRUCTURE TIDY[32] in PLATON.[33] Crystal structure data and refinement details for each compound are provided in Table 1 and in Supporting Information.

Optical Studies. Single-crystal absorption spectra were obtained at 298 K on a Hitachi U-6000 Microscopic FT spectrophotometer mounted on an Olympus BH2-UMA microscope. Crystals of $BaU(PS_4)_2$ and $SrU(PS_4)_2$ were placed on a glass slide and positioned over the light source where the transmitted light was recorded from above. The background signal of the glass slide was subtracted from the collected intensity. The reflectance data were converted to absorption data according to the Kubelka−Munk equation $\alpha/S = (1 - R)^2/(2R)$, where R is the reflectance and α and S are the absorption and scattering coefficients, respectively.[34]

Optical diffuse reflectance measurements were performed at 298 K on $SrTh(PS_4)_2$ using a computer-controlled Shimadzu UV-3101PC double beam, double monochromator spectrophotometer equipped with an integrating sphere. Single crystals of $SrTh(PS_4)_2$ were ground to a fine powder and spread on a compacted surface of powdered $BaSO_4$ that was used as a 100% reflectance standard material.

Theoretical Calculations. These have been performed with the VASP (Vienna ab Initio Simulation Package) code[35,36] and the projector augmented wave method,[37] implementing spin-polarized density functional theory.[38,39] In order to obtain realistic band gaps, the HSE (Heyd, Scuseria, Ernzerhof) functional[40−42] was used. The experimental cell parameters and atomic positions were used. For $BaU(PS_4)_2$ and $SrU(PS_4)_2$, the total energy of the various possible magnetic orders that can take place in a crystal cell were compared, and the one with the lowest total energy was retained as the ground state. $SrTh(PS_4)_2$ is not magnetic. A k-point mesh of 2 × 2 × 2 and the default cutoff for the wave function were used as the numerical parameters in the calculations.

Table 1. Crystallographic Data and Structure Refinement Details for $SrU(PS_4)_2$, $BaU(PS_4)_2$, and $SrTh(PS_4)_2$[a]

	$SrU(PS_4)_2$	$BaU(PS_4)_2$	$SrTh(PS_4)_2$
fw (g mol^{-1})	644.07	693.79	638.08
a (Å)	10.9717(2)	11.1405(4)	11.0284(12)
c (Å)	9.5734(2)	9.6604(5)	9.6725(9)
V (Å^3)	1152.43(5)	1198.96(11)	1176.4(3)
λ (Å)	0.710 73	1.541 78	0.710 73
ρ (g cm^{-3})	3.712	3.844	3.603
μ (mm^{-1})	20.331	78.24	18.795
$R(F)^b$	0.013	0.024	0.010
$R_w(F_o^2)^c$	0.030	0.063	0.028

[a]For all structures, space group D_{4h}^{13}-$P4_2/mbc$, T = 100(2) K, Z = 4. [b]$R(F) = \sum||F_o| - |F_c||/\sum|F_o|$ for $F_o^2 > 2\sigma(F_o^2)$. [c]$R_w(F_o^2) = \{\sum[w(F_o^2 - F_c^2)^2]/\sum wF_o^4\}^{1/2}$. For $F_o^2 < 0$, $w^{-1} = \sigma^2(F_o^2)$; for $F_o^2 \geq 0$, $w^{-1} = \sigma^2(F_o^2) + (qF_o^2)^2$ where q = 0.0127 for $SrU(PS_4)_2$, 0.0437 for $BaU(PS_4)_2$, and 0.0116 for $SrTh(PS_4)_2$.

RESULTS

Syntheses. The reactions that resulted in orange needles of $SrU(PS_4)_2$ and yellow needles of $SrTh(PS_4)_2$ in about 70 wt % yield involved Sr, U or Th, P_2S_5, and S at 1123 K. Several unsuccessful attempts were made to improve the yields. A similar reaction involving Ba and U at 1053 K provided orange needles of $BaU(PS_4)_2$ in only about 10 wt % yield, with the major product being black blocks of UP_2S_7.[13,14]

Crystal Structures. The isostructural compounds $SrU(PS_4)_2$, $BaU(PS_4)_2$, and $SrTh(PS_4)_2$ crystallize in a new structure type with four formula units per cell in the tetragonal space group D_{4h}^{13}-$P4_2/mbc$ (Table 1). The asymmetric unit contains one An (site symmetry $\bar{4}$..), one Ak (2.22), one P (m..), and three S atoms (S1(1), S2 (m..), S3(m..)). A general view of the structure down the c-axis is shown in Figure 1, and selected metrical data are given in Table 2. The crystal structure consists of infinite one-dimensional chains of $^1_\infty[An(PS_4)_2^{2-}]$ anions oriented along the c-axis (Figure 2) and Ak^{2+} cations. Each An atom is surrounded by eight S atoms in a bicapped trigonal-prismatic arrangement, and each P atom is tetrahedrally coordinated to four S atoms. The An atoms are connected to each other by the sharing of two S atoms along the c-axis. Two PS_4 tetrahedral units share one edge with each An polyhedron (Figure 2). The Ak cations are situated in pseudochannels and are connected to eight S atoms. The interplay among $^1_\infty[An(PS_4)_2^{2-}]$ chains is shown in Figure 3.

The construction of the $^1_\infty[An(PS_4)_2^{2-}]$ chains is very similar to that found in the structure of UP_2S_6[13] where each An atom is coordinated to eight S atoms provided by four PS_4 groups. However, the structure of UP_2S_6 is three-dimensional owing to the replacement of two PS_4 groups by one P_2S_6 group.

In the present $AkAn(PS_4)_2$ structures the Ak and An atoms are ordered and in two different independent crystallographic sites. Similarly, the structures of the $BaAn(PO_4)_2$[43] compounds (An = Th, Np) contain ordered Ba and An sites. Usually,

DOI: 10.1021/acs.inorgchem.5b00071
Inorg. Chem. 2015, 54, 2970−2975

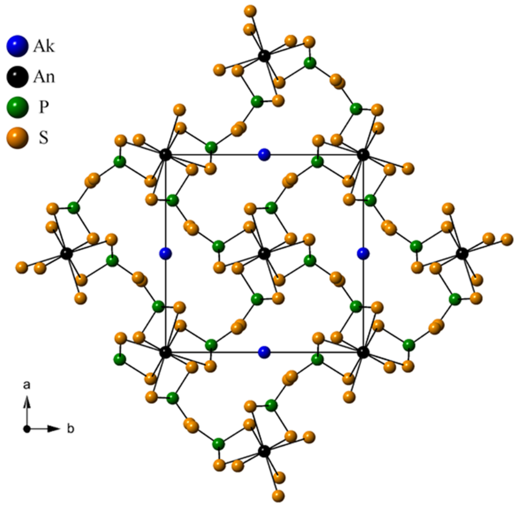

Figure 1. General view down the *c*-axis of the $AkAn(PS_4)_2$ structure.

Table 2. Interatomic Lengths (Å) in $SrU(PS_4)_2$, $BaU(PS_4)_2$, and $SrTh(PS_4)_2$^{a}

distance (Å)	$SrU(PS_4)_2$	$BaU(PS_4)_2$	$SrTh(PS_4)_2$
An1−S1	2.754(1) × 4	2.747(1) × 4	2.820(1) × 4
An1−S2	2.947(1) × 4	2.960(1) × 4	2.988(1) × 4
P1−S3	2.000(1)	1.996(2)	1.999(1)
P1−S1	2.045(1) × 2	2.051(1) × 2	2.043(1) × 2
P1−S2	2.063(1)	2.059(2)	2.069(1)
Ak1−S3	3.077(1) × 4	3.169(1) × 4	3.093(1) × 4
Ak1−S1	3.131(1) × 4	3.232(1) × 4	3.108(1) × 4

^{a}To facilitate comparisons all distances have been rounded from CIF files in Supporting Information.

however, the Ak/An atoms are disordered in the same site, and the resultant structures belong to the cheralite family ($Ak^{II}_{1-x}An^{IV}_xPO_4$) derived from the monazite structure type $LnPO_4$.[1,3]

Oxidation States. There are no S−S single bonds in these structures so charge balance is achieved with Ak^{2+}, U^{4+} or Th^{4+}, P^{5+}, and S^{2-}. The U−S distances in $SrU(PS_4)_2$ (2.754(1) and 2.947(4) Å) and $BaU(PS_4)_2$ (2.747(1) and 2.960(1) Å) are in agreement with those in known related compounds containing eight-coordinated U^{4+} such as $Ba_2U(S_2)_2S_2$ (2.7337(2) to 2.8199(7) Å)[44] and $FeUS_3$ (2.755(1) to 2.977(1) Å).[45] The Th−S distances of 2.820(1) and 2.988(1) Å are comparable with those of 2.844(2) to 2.968(1) Å found in $K_{10}Th_3(P_2S_7)_4(PS_4)_2$.[18] In the present structures, the P−S distances of 2.000(1) to 2.063(1) Å for $SrU(PS_4)_2$, 1.996(2) to 2.059(2) Å for $BaU(PS_4)_2$, and 1.999(1) to 2.069(1) Å for $SrTh(PS_4)_2$ are typical of PS_4^{3-}, for example in $U_3(PS_4)_4$ (2.037(2) to 2.039(2) Å),[13] $Np(PS_4)$ (2.0340(7) to 2.0361(7) Å),[15] $K_3Pu(PS_4)_2$ (2.000(3) to 2.068(3) Å),[19] $CsLiU(PS_4)_2$ (2.024(2) to 2.047(2) Å),[17] $K_{11}U_7(PS_4)_{13}$ (1.930(8) to 2.226(9) Å),[16] and $Rb_{11}U_7(PS_4)_{13}$ (1.948(8) to 2.081(8) Å).[16]

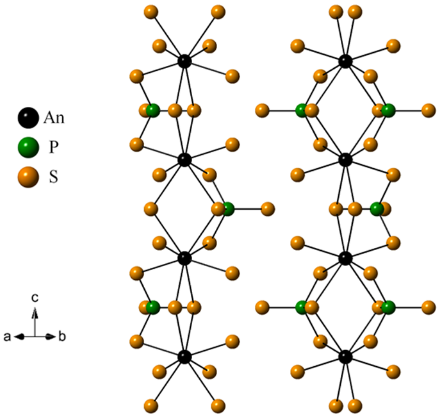

Figure 3. Arrangement among the $^1_\infty[An(PS_4)_2{}^{2-}]$ chains.

In addition, the use of the empirical Bond Valence Sum analysis[46] as implanted in PLATON[33] provided the following valences for the cations: $SrU(PS_4)_2$, U 3.67, Sr 2.00; $BaU(PS_4)_2$, U 3.66, Ba 2.49; and $SrTh(PS_4)_2$, Th 4.02, Sr 2.01. The method is strictly empirical, and we report the valences only in support of the conclusions based on the analysis of the interatomic distances.

Optical Properties. A single-crystal absorption spectrum collected for $SrU(PS_4)_2$ at 298 K shows a broad band gap transition between 1.8 and 2.4 eV with an onset value of 2.05(2) eV (Figure 4, left). α^2 should vary linearly with energy for a direct transition whereas $\alpha^{1/2}$ should vary linearly for an indirect transition, where α is the absorbance. The plots of α^2 and $\alpha^{1/2}$ (Figure 4, right) lead to values of 2.13(2) and 1.99(2)

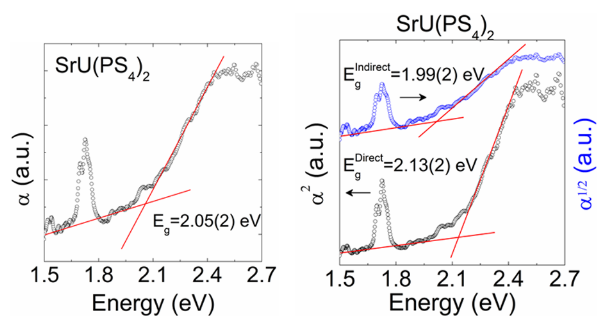

Figure 4. Absorption spectrum of a single crystal of $SrU(PS_4)_2$ measured at 298 K (left), and the plots of α^2 and $\alpha^{1/2}$ vs energy (right).

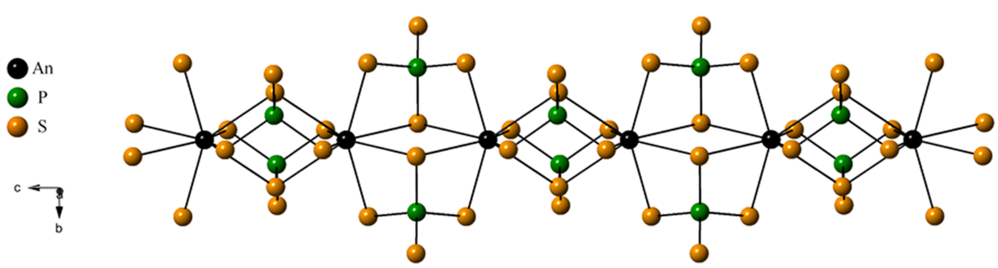

Figure 2. Infinite $^1_\infty[An(PS_4)_2{}^{2-}]$ chains viewed along the *c*-axis.

DOI: 10.1021/acs.inorgchem.5b00071
Inorg. Chem. 2015, 54, 2970−2975

eV for the direct and indirect transitions, consistent with the orange color of the crystals. The shapes of these curves favor the direct transition. Similar analyses of the absorption data collected on a single crystal of $BaU(PS_4)_2$ (Figure 5, left) show

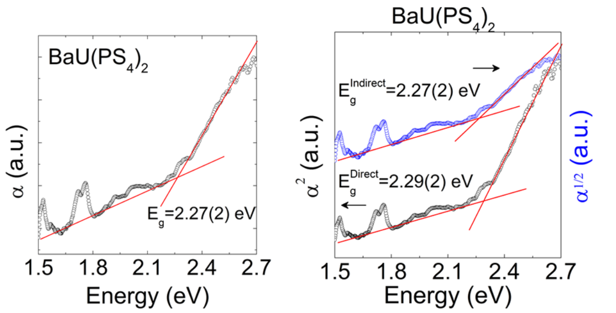

Figure 5. Absorption spectrum of a single crystal of $BaU(PS_4)_2$ measured at 298 K (left) and the plots of α^2 and $\alpha^{1/2}$ vs energy (right).

the direct and indirect gaps of around 2.28(2) eV (Figure 5, right). $SrTh(PS_4)_2$ has a band gap of 3.02(2) eV (Figure 6).

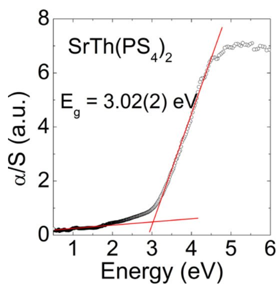

Figure 6. Diffuse reflectance spectrum of $SrTh(PS_4)_2$ measured at 298 K.

However, the diffuse reflectance measurement on $SrTh(PS_4)_2$ powder does not allow further analysis of the nature of the gap because absorbance is not measured directly in a diffuse reflectance geometry.

DFT Calculations. The densities of states (DOS) of $SrU(PS_4)_2$ and $BaU(PS_4)_2$ are presented in Figures 7 and 8, respectively. Both compounds are found to be antiferromagnetic, as seen from the symmetric total density of states. The two compounds have very similar electronic structures, with direct band gaps of 2.7 eV in comparison with the experimental values of 1.99(2) eV for $SrU(PS_4)_2$ and 2.28(2) eV for $BaU(PS_4)_2$. The magnetic moment of the U atoms induces a small spin polarization on the neighboring atoms, which can be best seen on the partial density of states of Sr or Ba. For each compound the top of the valence states is made of S-p and U-f states, while the bottom of the conduction states correspond mainly to U-f states. The total and partial DOS for $SrTh(PS_4)_2$ are shown in Figure 9. $SrTh(PS_4)_2$ is not magnetic, and the calculated band gap is 3.2 eV, in reasonable agreement with the measured value of 3.02 eV. As seen from the partial density of states, the top of the valence states corresponds mainly of p states from the different S atoms, while the bottom of the conduction bands is made of Th-d and Th-f states, with a contribution of P-s states.

■ CONCLUSIONS

Three new actinide thiophosphates, $SrU(PS_4)_2$, $BaU(PS_4)_2$, and $SrTh(PS_4)_2$, have been synthesized by high-temperature solid-state methods, and their crystal structures were determined from single-crystal X-ray diffraction studies. These three isostructural compounds crystallize in a new structure type in space group D_{4h}^{13}-$P4_2/mbc$ of the tetragonal system. Their crystal structures feature infinite one-dimensional chains of $^1_\infty[An(PS_4)_2{}^{2-}]$ anions (An = U or Th). Each An atom is coordinated by eight S atoms in a bicapped trigonal prism, and each P atom is tetrahedrally bonded to four S atoms. All three

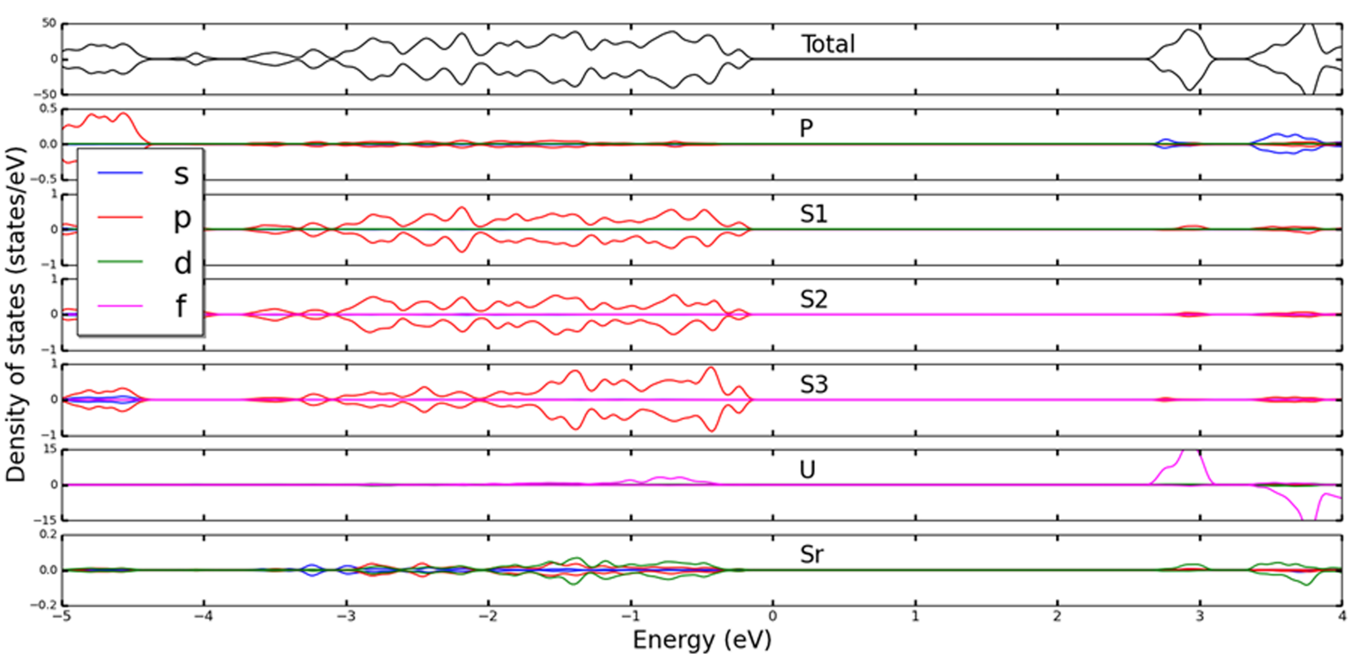

Figure 7. Total (upper plot) and partial density of states (lower plots) of $SrU(PS_4)_2$. For each atom, the PDOS is projected onto the relevant orbitals. The Fermi level is set at 0.

DOI: 10.1021/acs.inorgchem.5b00071
Inorg. Chem. 2015, 54, 2970−2975

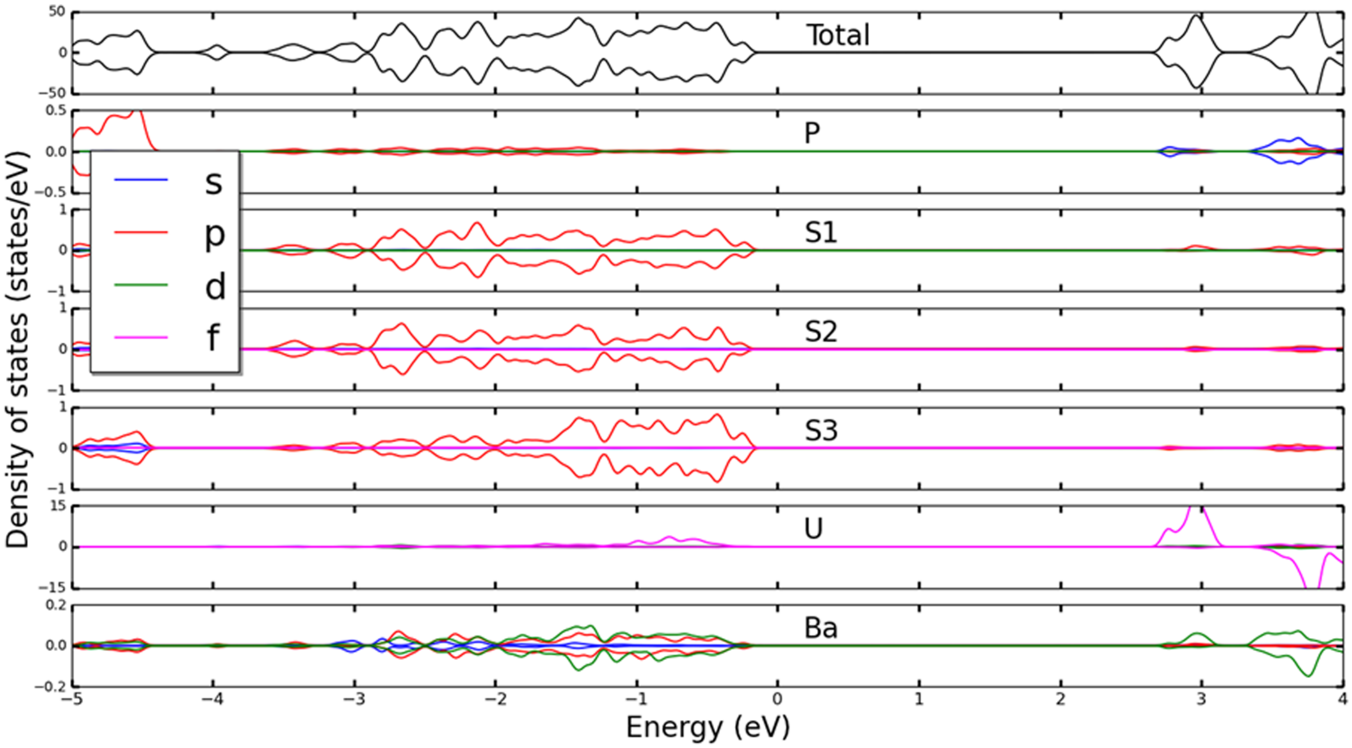

Figure 8. Total (upper plot) and partial density of states (lower plots) of $BaU(PS_4)_2$. For each atom, the PDOS is projected onto the relevant orbitals. The Fermi level is set at 0.

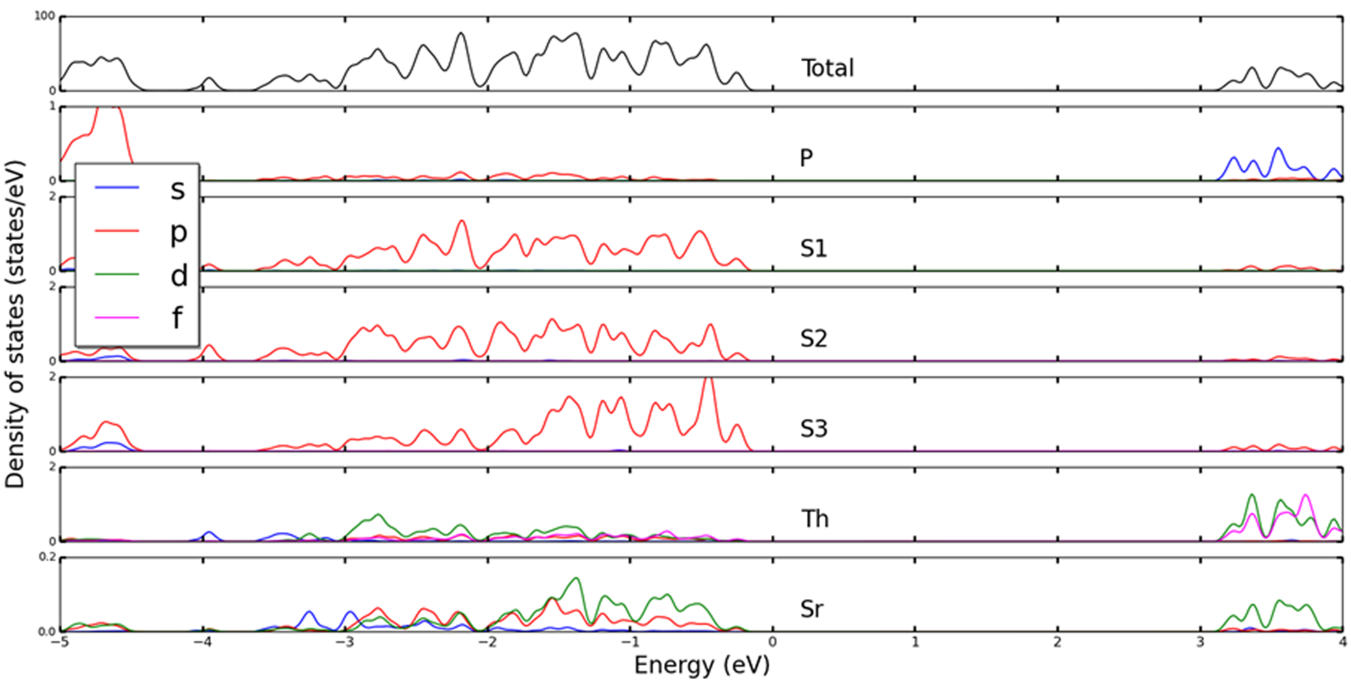

Figure 9. Total (upper plot) and partial density of states (lower plots) of $SrTh(PS_4)_2$. For each atom, the PDOS is projected onto the relevant orbitals. The Fermi level is set at 0.

compounds are readily charge balanced as $Ak^{2+}An^{4+}(P^{5+}(S^{2-})_4)_2$. These three compounds represent the first examples of actinides thiophosphates having alkaline-earths in their structures. They exhibit ordered positioning of Ak and An atoms, as observed previously in the $BaAn(PO_4)_2$ structures. Most oxides are derived from the monazite structure type and contain disordered Ak/An sites.

Optical measurements on single crystals of $SrU(PS_4)_2$ and $BaU(PS_4)_2$ as well as ground single crystals of $SrTh(PS_4)_2$ give band gaps of $SrU(PS_4)_2$ (2.13(2) (direct), 1.99(2) (indirect)), $BaU(PS_4)_2$ (2.28(2)), and $SrTh(PS_4)_2$ (3.2(2) eV) that are consistent with their colors and with DFT calculations. These calculations using the HSE functional indicate very similar electronic structures for $SrU(PS_4)_2$ and $BaU(PS_4)_2$ with band

DOI: 10.1021/acs.inorgchem.5b00071
Inorg. Chem. 2015, 54, 2970−2975

gaps of 2.7 eV and predict that both compounds are antiferromagnetic.

■ ASSOCIATED CONTENT

Supporting Information

Crystallographic files in CIF format for $SrU(PS_4)_2$, $BaU(PS_4)_2$, and $SrTh(PS_4)_2$. This material is available free of charge via the Internet at http://pubs.acs.org.

■ AUTHOR INFORMATION

Corresponding Author

*E-mail: ibers@chem.northwestern.edu.

Notes

The authors declare no competing financial interest.

■ ACKNOWLEDGMENTS

Use was made of the IMSERC X-ray Facility at Northwestern University, supported by the International Institute of Nanotechnology (IIN). S.L. acknowledges HPC resources from GENCI-CCRT/CINES (Grant x2014-085106). C.D.M. was supported by the U.S. Department of Energy, Office of Basic Energy Sciences under contract no. DE-AC02-06CH11357

■ REFERENCES

(1) Dacheux, N.; Clavier, N.; Podor, R. *Am. Mineral.* **2013**, *98*, 833−847.
(2) Deschanels, X.; Seydoux-Guillaume, A. M.; Magnin, V.; Mesbah, A.; Tribet, M.; Moloney, M. P.; Serruys, Y.; Peuget, S. *J. Nucl. Mater.* **2014**, *448*, 184−194.
(3) Clavier, N.; Podor, R.; Dacheux, N. *J. Eur. Ceram. Soc.* **2011**, *31*, 941−976.
(4) Clavier, N.; Dacheux, N.; Martinez, P.; Brandel, V.; Podor, R.; Le Coustumer, P. *J. Nucl. Mater.* **2004**, *335*, 397−409.
(5) Clavier, N.; Dacheux, N.; Martinez, P.; Du Fou de Kerdaniel, E.; Aranda, L.; Podor, R. *Chem. Mater.* **2004**, *16*, 3357−3366.
(6) Bénard, P.; Louër, D.; Dacheux, N.; Brandel, V.; Genet, M. *Chem. Mater.* **1994**, *6*, 1049−1058.
(7) Podor, R.; François, M.; Dacheux, N. *J. Solid State Chem.* **2003**, *172*, 66−72.
(8) Bénard, P.; Brandel, V.; Dacheux, N.; Jaulmes, S.; Launay, S.; Lindecker, C.; Genet, M.; Louër, D.; Quarton, M. *Chem. Mater.* **1996**, *8*, 181−188.
(9) Wallez, G.; Raison, P. E.; Dacheux, N.; Clavier, N.; Bykov, D.; Delevoye, L.; Popa, K.; Bregiroux, D.; Fitch, A. N.; Konings, R. J. M. *Inorg. Chem.* **2012**, *51*, 4314−4322.
(10) Baskin, Y.; Shalek, P. D. *J. Am. Ceram. Soc.* **1969**, *52*, 341−342.
(11) Kaczorowski, D.; Noël, H.; Potel, M.; Zygmunt, A. *J. Phys. Chem. Solids* **1994**, *55*, 1363−1367.
(12) Simon, A.; Peters, K.; Peters, E.-M. *Z. Anorg. Allg. Chem.* **1982**, *491*, 295−300.
(13) Neuhausen, C.; Hatscher, S. T.; Panthofer, M.; Urland, W.; Tremel, W. *Z. Anorg. Allg. Chem.* **2013**, *639*, 2836−2845.
(14) Babo, J.-M.; Jouffret, L.; Lin, J.; Villa, E. M.; Albrecht-Schmitt, T. E. *Inorg. Chem.* **2013**, *52*, 7747−7751.
(15) Jin, G.-B.; Skanthakumar, S.; Haire, R. G.; Soderholm, L.; Ibers, J. A. *Inorg. Chem.* **2011**, *50*, 1084−1088.
(16) Gieck, C.; Tremel, W. *Chem.—Eur. J.* **2002**, *8*, 2980−2987.
(17) Neuhausen, C.; Rocker, F.; Tremel, W. *Z. Anorg. Allg. Chem.* **2012**, *638*, 405−410.
(18) Hess, R. F.; Abney, K. D.; Burris, J. L.; Hochheimer, H. D.; Dorhout, P. K. *Inorg. Chem.* **2001**, *40*, 2851−2859.
(19) Hess, R. H.; Gordon, P. L.; Tait, C. D.; Abney, K. D.; Dorhout, P. K. *J. Am. Chem. Soc.* **2002**, *124*, 1327−1333.
(20) Chan, B. C.; Hess, R. F.; Feng, P. L.; Abney, K. D.; Dorhout, P. K. *Inorg. Chem.* **2005**, *44*, 2106−2113.
(21) Babo, J.-M.; Diefenbach, K.; Albrecht-Schmitt, T. *Inorg. Chem.* **2014**, *53*, 3540−3545.
(22) Chondroudis, K.; Kanatzidis, M. G. *Inorg. Chem.* **1998**, *37*, 2848−2849.
(23) Gieck, C.; Rocker, F.; Ksenofontov, V.; Gütlich, P.; Tremel, W. *Angew. Chem., Int. Ed.* **2001**, *40*, 908−911.
(24) Wu, Y.; Bensch, W. *Inorg. Chem.* **2007**, *46*, 6170−6177.
(25) Cody, J. A.; Finch, K. B.; Reynders, G. J.; Alexander, G. C. B.; Lim, H. G.; Nather, C.; Bensch, W. *Inorg. Chem.* **2012**, *51*, 13357−13362.
(26) Bugaris, D. E.; Ibers, J. A. *J. Solid State Chem.* **2008**, *181*, 3189−3193.
(27) Haneveld, A. J. K.; Jellinek, F. *J. Less-Common Met.* **1969**, *18*, 123−129.
(28) Helbing, R.; Feigelson, R. S. *J. Cryst. Growth* **1994**, *137*, 150−154.
(29) Bruker. *APEX2 Version 2009.5-1 Data Collection and Processing Software*; Bruker Analytical X-Ray Instruments, Inc.: Madison, WI, 2009.
(30) Sheldrick, G. M. *SADABS*; Department of Structural Chemistry, University of Göttingen: Göttingen, Germany, 2008.
(31) Sheldrick, G. M. *Acta Crystallogr., Sect. A* **2008**, *64*, 112−122.
(32) Gelato, L. M.; Parthé, E. *J. Appl. Crystallogr.* **1987**, *20*, 139−143.
(33) Spek, A. L. *PLATON, A Multipurpose Crystallographic Tool*; Utrecht University: Utrecht, The Netherlands, 2014.
(34) McCarthy, T. J.; Ngeyi, S.-P.; Liao, J.-H.; DeGroot, D. C.; Hogan, T.; Kannewurf, C. R.; Kanatzidis, M. G. *Chem. Mater.* **1993**, *5*, 331−340.
(35) Kresse, G.; Forthmüller, J. *Comput. Mater. Sci.* **1996**, *6*, 15−50.
(36) Kresse, G.; Joubert, D. *Phys. Rev. B* **1999**, *59*, 1758−1775.
(37) Blöchl, P. E. *Phys. Rev. B* **1994**, *50*, 17953−17979.
(38) Kohn, W.; Sham, L. J. *Phys. Rev.* **1965**, *140*, 1133−1138.
(39) Hohenberg, P.; Kohn, W. *Phys. Rev.* **1964**, *136*, 864−871.
(40) Heyd, J.; Scuseria, G. E.; Ernzerhof, M. *J. Chem. Phys.* **2003**, *118*, 8207−8215.
(41) Heyd, J.; Scuseria, G. E.; Ernzerhot, M. *J. Chem. Phys.* **2006**, *124*, 219906-1.
(42) Borovik-Romanov, A. S.; Grimmer, H. In *International Tables for Crystallography*; Authier, A., Ed.; International Union of Crystallography: Chester, U.K., 2006; Vol. *D*, pp 105−149.
(43) Wallez, G.; Bregiroux, D.; Popa, K.; Raison, P. E.; Apostolidis, C.; Lindqvist-Reis, P.; Konings, R. J. M.; Popa, A. F. *Eur. J. Inorg. Chem.* **2011**, *2011*, 110−115.
(44) Mesbah, A.; Ringe, E.; Lebègue, S.; Van Duyne, R. P.; Ibers, J. A. *Inorg. Chem.* **2012**, *51*, 13390−13395.
(45) Jin, G. B.; Ringe, E.; Long, G. J.; Grandjean, F.; Sougrati, M. T.; Choi, E. S.; Wells, D. M.; Balasubramanian, M.; Ibers, J. A. *Inorg. Chem.* **2010**, *49*, 10455−10467.
(46) Brown, I. D. *The Chemical Bond in Inorganic Chemistry, The Bond Valence Model*; Oxford University Press: New York, 2002.

DOI: 10.1021/acs.inorgchem.5b00071
Inorg. Chem. 2015, 54, 2970−2975